We are IntechOpen,
the world's leading publisher of Open Access books
Built by scientists, for scientists

6,900
Open access books available

185,000
International authors and editors

200M
Downloads

154
Countries delivered to

Our authors are among the

TOP 1%
most cited scientists

12.2%
Contributors from top 500 universities

CLARIVATE ANALYTICS
BOOK CITATION INDEX
INDEXED

WEB OF SCIENCE™

Selection of our books indexed in the Book Citation Index
in Web of Science™ Core Collection (BKCI)

Interested in publishing with us?
Contact book.department@intechopen.com

Numbers displayed above are based on latest data collected.
For more information visit www.intechopen.com

Finite Element Analysis of the Stress on the Implant-Bone Interface of Dental Implants with Different Structures

Liangjian Chen

Additional information is available at the end of the chapter

1. Introduction

Titanium and titanium alloys have become the preferred materials for dental implants owing to their good biocompatibility, excellent corrosion resistance and suitable mechanical properties. However, the existing titanium implants still have several drawbacks. Firstly, the bonding strength at the interface between the implant and the bone is not high enough and the biological fixation has not been achieved. Secondly, there exist mismatches between the elastic modulus of the implant and of the bone. A stress shielding or concentration can be easily induced on the interface and results in a potential risk to the long-term stability of the implant. The success or failure of an implant is determined by the manner how the stresses at the bone-implant interface are transferred to the surrounding bones [1,2]. The mandible has structural characteristic of an outer layer of dense cortical bone and an inner layer of porous cancellous bone. The elastic modulus and mechanical properties of cortical bones are different from those of cancellous bones. Nevertheless, current dental implants are mainly fabricated using dense titanium and titanium alloys, which have no features representing the difference between the inner and outer layers of the mandible or that between their elastic modulus. And therefore, the incompatibility of the mechanical properties between the implant and the bone was encountered. The use of porous metal implants for medical applications has two main advantages. One is the similar elastic modulus to the bone, which helps to prevent the stress shielding effect at the bone interfaces. The other is that it can provide a structural condition for the bone ingrowth to achieve biological fixation [3,4]. However, the low mechanical strength limits their further applications in the implanting industry. In this study, according to the structural characteristics of the mandible and the clinical requirements for the implant mechanical properties, a novel bio-mimetic design of implant is proposed for the titanium implants, which composes of a cortical bone zone with

a dense structure and a cancellous bone zone with a porous outer layer and a dense core, as well as another three implants with different structures.

The finite element method is one of the most frequently used methods in stress analysis in both industry and science[5]. Three-dimensional (3-D) finite element analysis (FEA) has been widely used for the quantitative evaluation of stresses on the implant and its surrounding bone[6,7]. Therefore, FEA was selected for use in this study to examine the effect of the structure and elastic modulus of dental implant on the stress distribution at implant-bone interface. The 3-D models of the designed implants were constructed and the finite element analyses were carried out using Ansys Workbench 10.0. The stress distributions on implant-bone interface were investigated under static loading condition in order to provide design guidelines for the development of new implants. At the same time,the stress distributions on implant-bone interface were investigated in both dynamic and static loading conditions, and the fatigue behaviors of the bio-mimetic implant were analyzed based on fatigue theories and the formulas, in order to provide theoretical basis for the development of new implants.

2. Material and methods

2.1. Structur of the biomimetic implant

The biomimetic implant comprised of two layers, including the porous layer of open connected pores, which can provide the structure for bone ingrowth and has mechanical properties similar to the surrounding bones. The dense core ensures that the mechanical properties of implant meet the requirements of clinical applications (Fig.1).
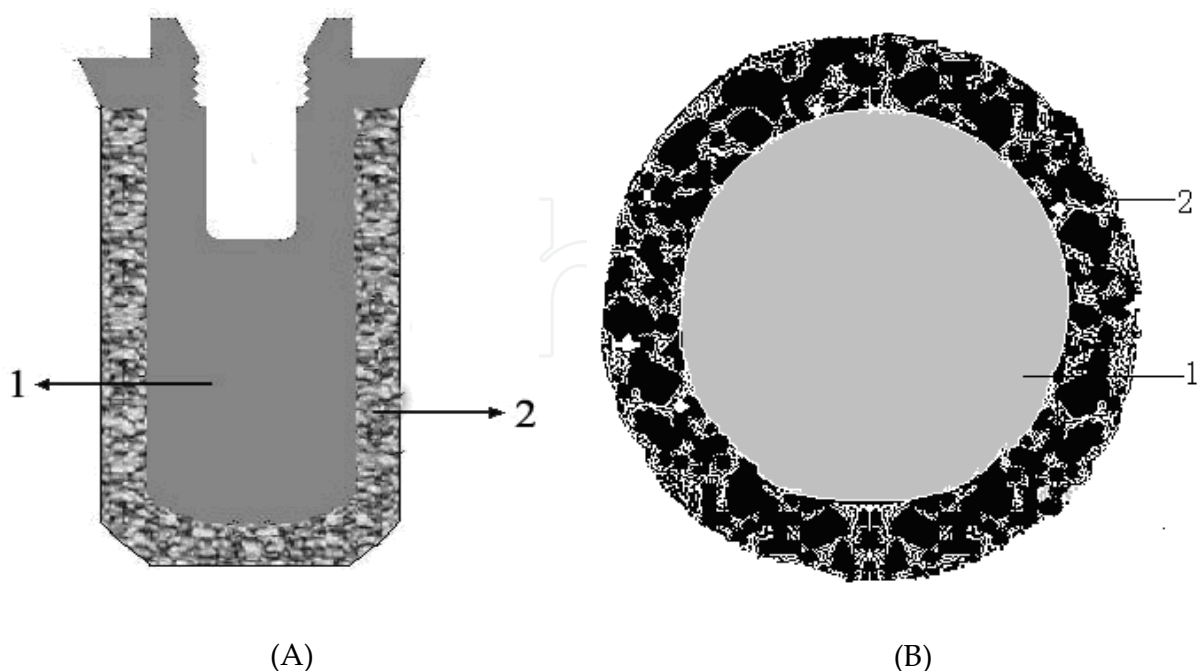

(A)   (B)

Figure 1. Structure of the bio-mimetic porous titanium implant. A:section plane, B : cross section, 1: dense core, 2: porous layer

2.2. CAD and finite element modeling of the elements

A 3-D model of a mandibular section of bone with a missing second premolar and its superstructures were used in this study. A mandibular bone model was selected according to the classification system of Lekholm and Zarb. Trabecular bone was modeled as a solid structure in cortical bone. A bone block with dimensions of 20×14×35mm, representing the section of the mandible in the second premolar region, was modeled. It consisted of a spongy center surrounded by cortical bone of 2 mm.

Four implants models with dimensions of d4.1 mm×12mm were selected in this study. Those implants and abutment were assumed to consist of the same material. Implant No.1 was dense with a high elastic modulus. Implant No.2 was a bio-mimetic with a high modulus in the cortical bone zone and low modulus-outer and high modulus-interior in the cancellous bone zone. Implant No.3 had a high modulus in the cortical bone zone and a low modulus in the cancellous bone zone. Implant No.4 had a whole lower elastic modulus. The elastic modulus of the dense titanium (high modulus) was set as 103.4GPa. The elastic modulus of implant No.1 (low modulus) was set as 40% of the dense titanium. To investigate the effect of elastic modulus on the interface stress, modulus in the low modulus zone varied in the range of 80%,40% ,10% and 1.3% of the modulus of the dense titanium, i.e.1370MPa. Mechanical properties of the implants were shown in Table 1.

The 3-D model of the implants was constructed by the CAD software Pro/E. The finite element analyses were carried out using Ansys Workbench 10.0. Tetrahedron elements in implant and bone corresponding to SOLID45 type elements in ANSYS element library with each node had three degrees of freedom. The finite element model is shown Fig.2 and Fig.3. The physical interactions at implant–bone interfaces during loading were taken into account through bonded surface-to-surface contact features of ANSYS. Numbers of nodes and elements of implant and bones were shown in Table 2.
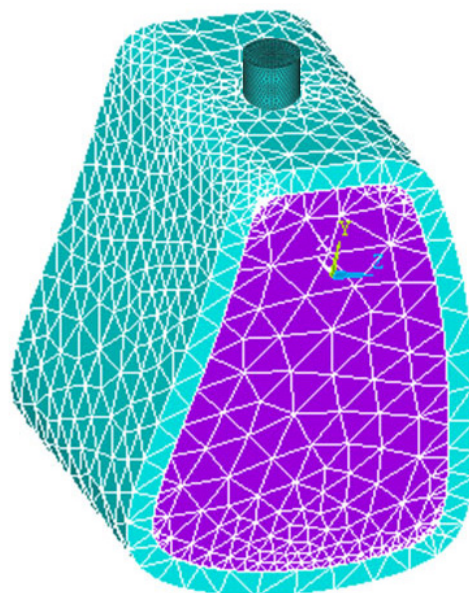
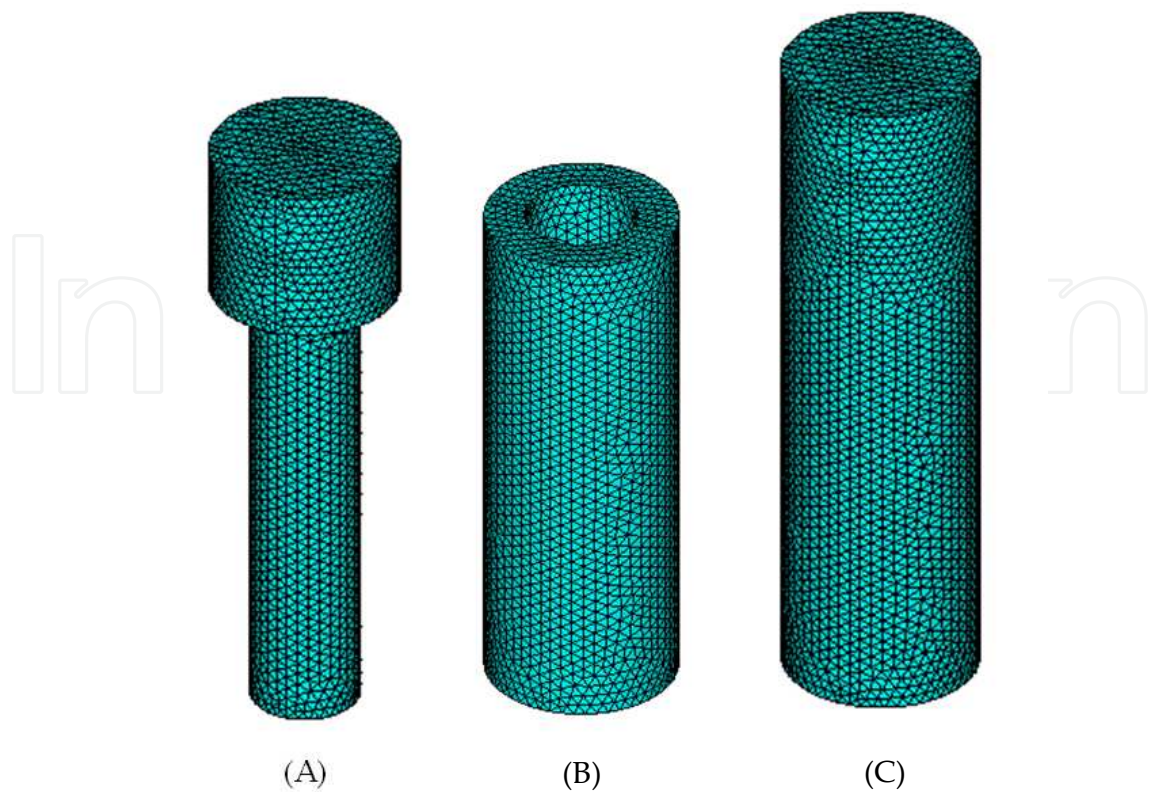

Figure 2. Finite element models of bone and implant

(A)   (B)   (C)

Figure 3. Finite element models of implant. A: dense body, B: porous layer, C: implant

Material	Elastic Modulus/GPa	Poisson ratio $,\upsilon$
Lower modulus titanium	41.36	0.35
Dense titanium	103.4	0.35
Cortical bone	13.70	0.30
Cancellous bone	1.37	0.30

Table 1. Mechanical properties of materials used in the study

Implants	Number of nodes		Number of elements	
	Dense	Porous	Dense	Porous
No.1 and No.4	15835	-	84828	-
No.2	8880	9186	45486	42926
No.3	3968	12313	20230	65703
Cortical bone	13329 -		65297 -	
Cancellous bone	- 5395		- 16324	

Table 2. Numbers of nodes and elements of implant and bones

2.3. Loads and boundary conditions

All materials were assumed to be homogenous, isotropic and linearly elastic. The bone-implant interfaces were assumed to be 100% osseointegrated. The sides and bottom of

cortical and cancellous bones were set to be completely constrained, and the boundary conditions were extended to the corresponding node. Multi-constraining was imposed on implant from bottom to top, in order to limit the freedom of the roots.

Static loading was loaded to evaluate the implant-bone model. The implants were assumed to be under an axial force of 50-300N and a lingual force of 25 N in the angle of approximately 45° to the occlusal plane .

Static and dynamic analyses of the implant need to consider and ensure the safety in the design. In the literature, implants are often worked according to the results of static analysis. Under the same masticatory forces, dynamic effects may add 10–20% more loads to implant than static effects. This must be taken into account to safeguard the fracture or fatigue failure of the implant. Therefore, using dynamic loading during the evaluation of a new implant is more reasonable. In the simulation of the normal chewing motion, forces close to the masticatory forces of normal adults were loaded to implant-bone model. Time dependent masticatory load was applied. Time history of the dynamic load components for 5 s is demonstrated in Fig. 4. These estimations were based on the assumption that an individual has three episodes of chewing per day, each 15 min in duration at a chewing rate of 60 cycles per minute (1 Hz). This is equivalent to 2700 chewing cycles per day or roughly 106 cycles per year.

The von Mises stresses were used as the key indicators to measure stress levels and evaluate the stress distribution at implant-bone interface, as well as the maximum stress values on cortical bone. The main indicators are: 1) stress distribution in axial at the implant-bone interface, and 2) the maximum von Misese stresses.
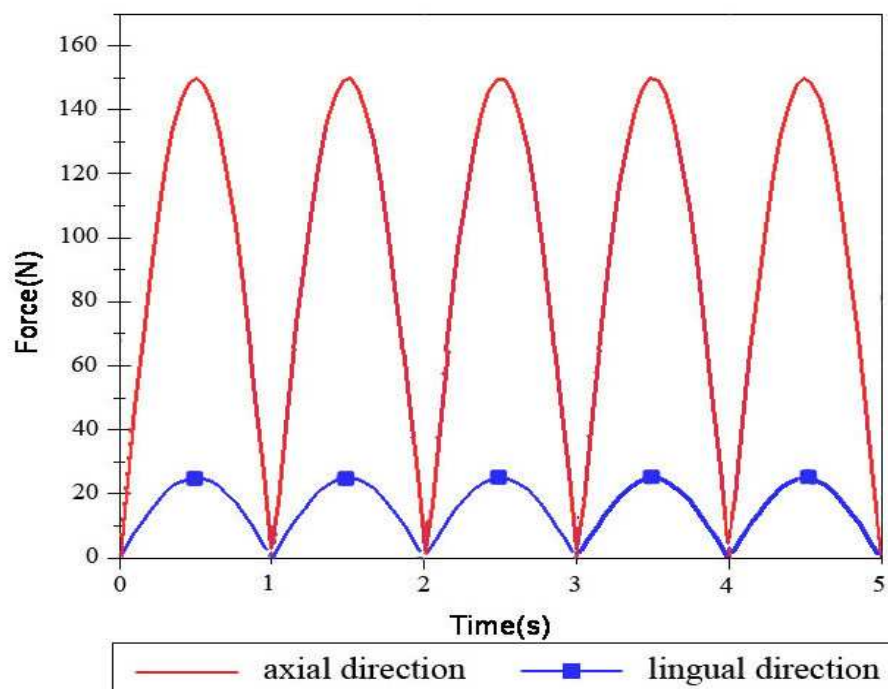

Figure 4. Dynamic loading in 5 seconds

2.4. Fatigue analysis

A good dental implant design should satisfy the maximum or an infinite fatigue life. This can only be ensured by physical testing or a fatigue analysis. In this study, the fatigue life of the dental implant was predicted using the finite element stress analysis with computer code of ANSYS/Workbench (ANSYS, 2003). Fatigue properties shown in Fig. 5 were used in fatigue calculations. Fig. 5 was known as S–N curves, showing fatigue properties of pure titanium in terms of alternating stress versus number of cycles. Fatigue life of prosthesis was calculated based on Goodman, Soderberg, Gerber and mean-stress fatigue theories which were illustrated in Table 3.

In Table 3, N indicates the safety factor for fatigue life in loading cycle, while Se is for endurance limit and Su is for ultimate tensile strength of the material. Mean stress σm and alternating stress σa are defined respectively as below, respectively.

$$\sigma_m = \frac{\sigma_{max} + \sigma_{min}}{2} \tag{1}$$

$$\sigma_a = \frac{\sigma_{max} - \sigma_{min}}{2} \tag{2}$$

Von Misses stresses obtained from finite element analyses are utilized in fatigue life calculations. All fatigue analyses were performed according to the infinite life criteria (i.e. N = 10^9 cycles).
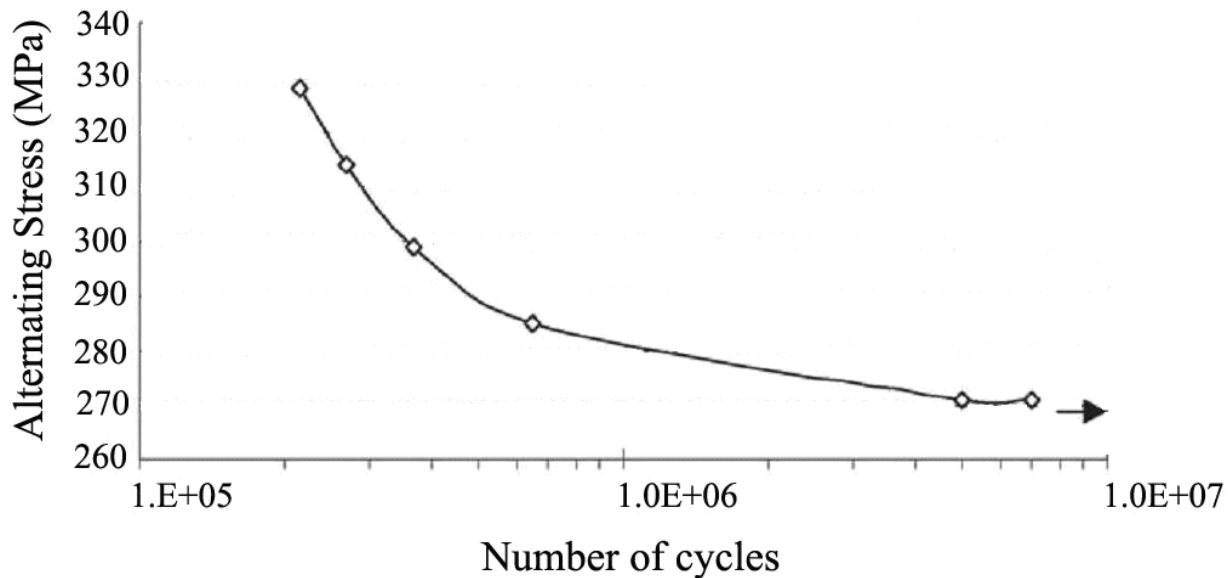

Figure 5. Fatigue curves (S-N curve) of pure titanium

Fatigue theories	Fatigue formulas
Goodman	$\left(\dfrac{\sigma_a}{S_e}\right)+\left(\dfrac{\sigma_m}{S_u}\right)=\dfrac{1}{N}$
Soderberg	$\left(\dfrac{\sigma_a}{S_e}\right)+\left(\dfrac{\sigma_m}{S_y}\right)=\dfrac{1}{N}$
Gerber	$\left(\dfrac{N\sigma_a}{S_e}\right)+\left(\dfrac{N\sigma_m}{S_u}\right)^2=1$

Table 3. Fatigue theories and formulas used in fatigue life predictions

3. Results

3.1. Stress distribution on implant-bone interface under static loading condition

3.1.1. The maximum stresses at implant-bone interface

Table 4 shows the maximum von Mises stresses of different structure implants. It can be seen that the interface stresses of implant No.3 are much higher than those of other implants. There is no obvious difference in the maximum stress between implant No.1 and No.4. Implant No.2 has the lowest maximum stress at both cancellous bone and root zone comparing with other implants. After the transferring of stress to the surrounding bones, the maximum stress in cortical bone is larger than that of cancellous bone in the surrounding bone tissue. Implant No.1 has the largest stress in cortical bone and No.3 has the largest stress in the root of cancellous bone.

Implants	Stress/MPa			
	Cortical bone interface	Cancellous bone interface	Cortical bone	Cancellous bone
No.1	23.434	12.553	11.668	1.456
No.2	23.451	8.261	9.685	1.525
No.3	33.532	15.77	8.419	4.845
No.4	23.453	14.482	9.012	1.799

Table 4. Maximum von Mises stresses of implants with different structures

3.1.2. Stress distribution at implant-bone interface of implants under static loading.

Figure 6 represents the stress distribution at the implant-bone interface in an axial direction. It can be seen that the maximum stresses of the implant No.1, 2 and 4 show no difference in the cortical bone zone and the maximum stress zone is located at the marginal zone of cortical bone. The maximum stress zone of implant No.3 is located at the interface between cortical and cancellous bones. The area of the high stress zone and the value of interface stress of the implant No.2 are the smallest in both the cancellous bone and its root apex.

Figure 7 represents the stress distribution in the cancellous bone zone of the implants. In all cases, there are high stress zones in the junction of the porous layer and the dense body. Among them, implant No.2 has the lowest interface stress. In the cancellous bone zone, the interface stress decreases from top to bottom, and increases at the root apex. And once again, No.2 has the lowest stress at the root apex, while No.3 has an obvious higher value than the others. The maximum stress exists at the bone interface of the implant No.1, which was 42.96% higher than that of implant No.2.

It was demonstrated that the structure of the implants has a predominate influence on the interface stress. Implant No.3 has a high trend to cause the stress concentration, while implant No.2 can efficiently reduce the interface stress, facilitating the transportation of the interface stress to the surrounding bones, avoiding the stress shielding and concentration, which is beneficial for the long time stability of the implants.
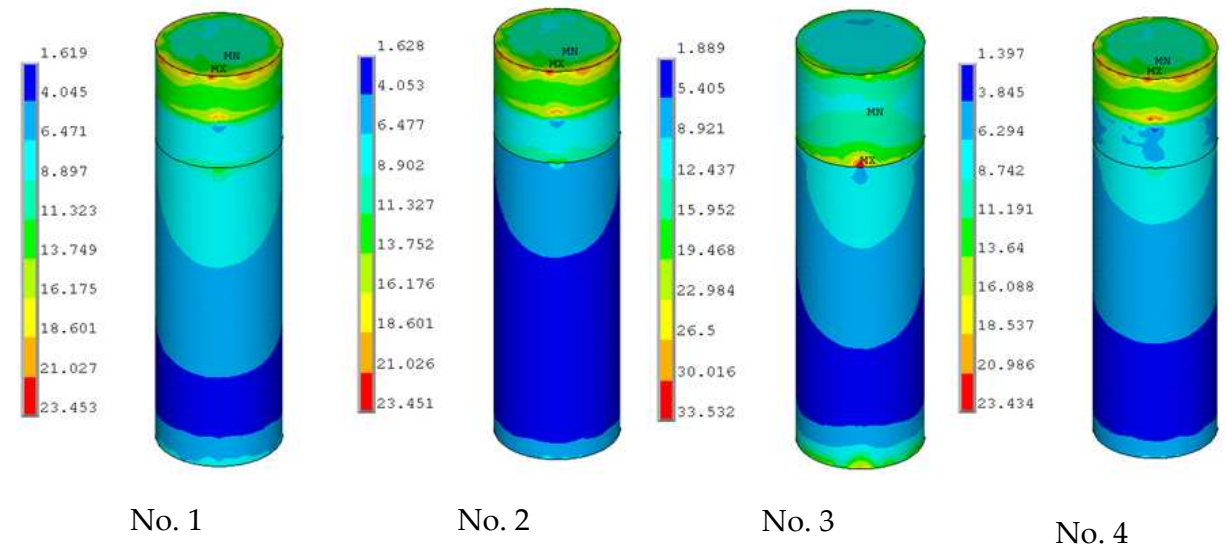

No. 1   No. 2   No. 3   No. 4

Figure 6. Stress distribution in axial direction at implant-bone interface of different structure implants

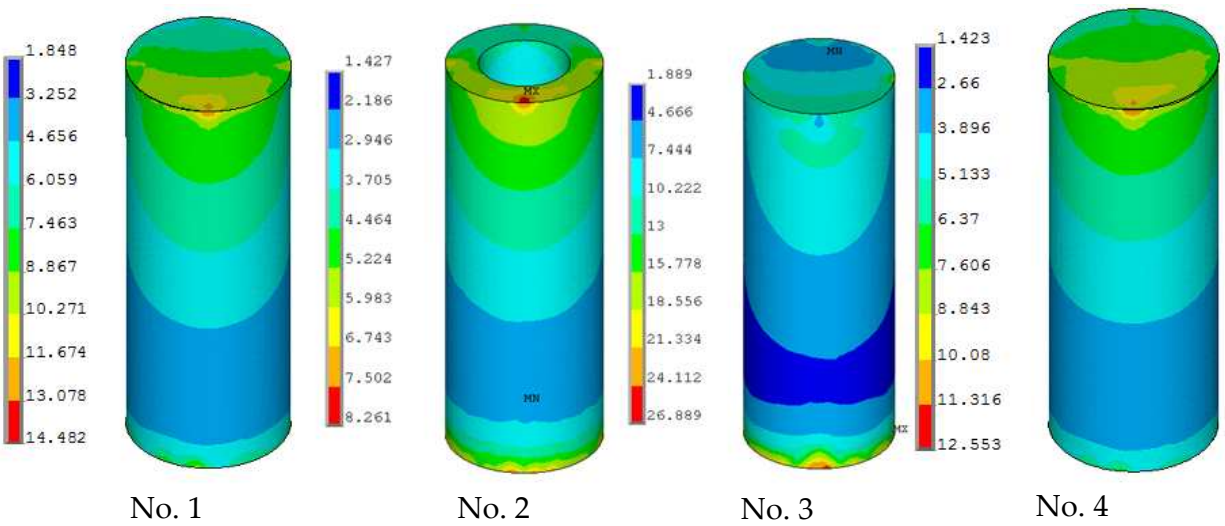No. 1   No. 2   No. 3   No. 4

Figure 7. Stress distribution in spongy bone zone of different structure implants

3.2. Effect of elastic modulus on the interface stress distribution of implant No.2

It was demonstrated that implant No.2 has the lowest interface stress. Thus, it is chosen to study the effect of elastic modulus of low modulus zone on the interface stress distribution at the interfaces. The elastic modulus in the low modulus zone varies in the range of 80%, 40%, 10% 1.3% of the modulus of the dense titanium, i.e.1370MPa. Table 8 shows that the interface stress in cancellous bone decreases with the decrease of the modulus of the low modulus layer, while there is no significant change in the cortical bone zone. For the interface stress of surrounding bones, it can be seen that the stress increases and that at the root apex of cancellous bone decreases with the decrease of the modulus of the low modulus layer.

Implants	Stress/MPa			
	Cortical bone interface	Cancellous bone interface	Cortical bone brink	Cancellous bone root apex
80%	23.452	12.725	9.172	1.739
40%	23.451	8.261	9.685	1.525
10%	23.451	3.733	11.224	1.094
1370MPa	23.443	2.216	12.304	1.351

Table 5. Maximum von Mises stresses of implants

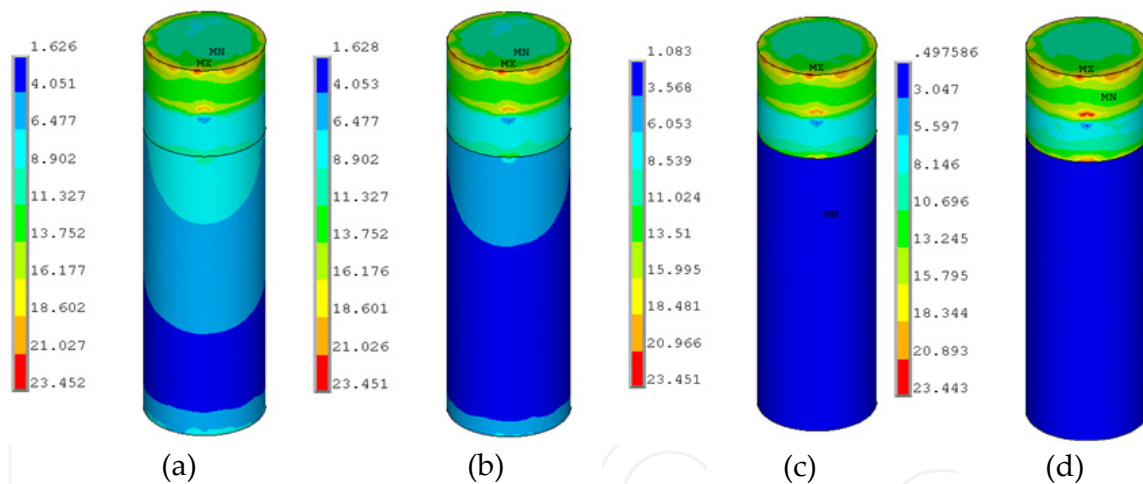(a)   (b)   (c)   (d)

Figure 8. Stress distribution of implant No.2 in axial direction at implant-bone interface: (a)80%; (b)40%; (c)10%; (d)1.3%

Figure 9 represents the stress distribution at the implant-bone interface in the axial direction. It can be seen that, under the same loading, a decrease of the modulus at low modulus layer has no significant influence on the interface stress of cortical bone. Figure 5 shows the stress distribution at the interface between implant No.2 and cancellous bone. The interface stress varies significantly with the change of the modulus of the low modulus layer. As the modulus of the low modulus layer decreases, the area of the high stress zone reduces, and the volume of the interface decreases dramatically. When the modulus of the low modulus layer reduces to 10% of the dense value, a uniform distribution of the interfacial stress without any high stress zone is obtained. For the specimens with the modulus of 1370MPa, the interface stress is 2.216MPa, 82.6% smaller than that of 80% ones. With the decrease of

the modulus, the interface stress between the dense core and the porous layer increases. Figure 10 represents the stress distribution in dense body of implants No.2. It can be seen that the high stress zone is located at the interface between the cortical bone and cancellous bone. For the specimens with the modulus of 10% of the dense ones, the maximum interfacial stress at the porous-dense core interface is 18.556MPa. And it reduced to 13.752MPa for those of 80% specimens.
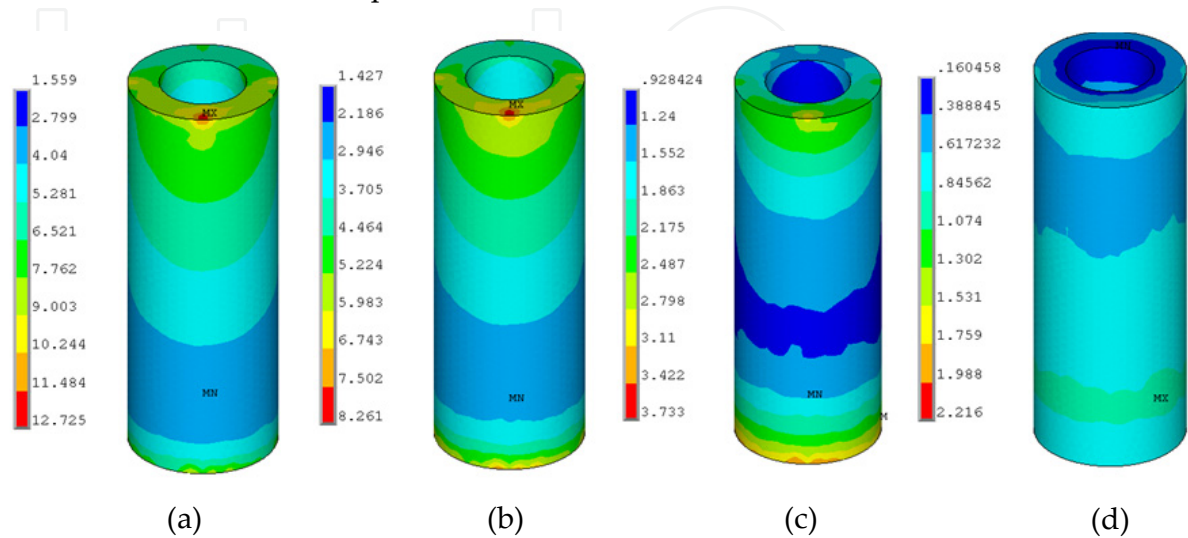

(a)   (b)   (c)   (d)

Figure 9. Stress distribution at interface between implant No.2 and cancellous bone: (a)80%; (b)40%; (c)10%; (d)1.3%

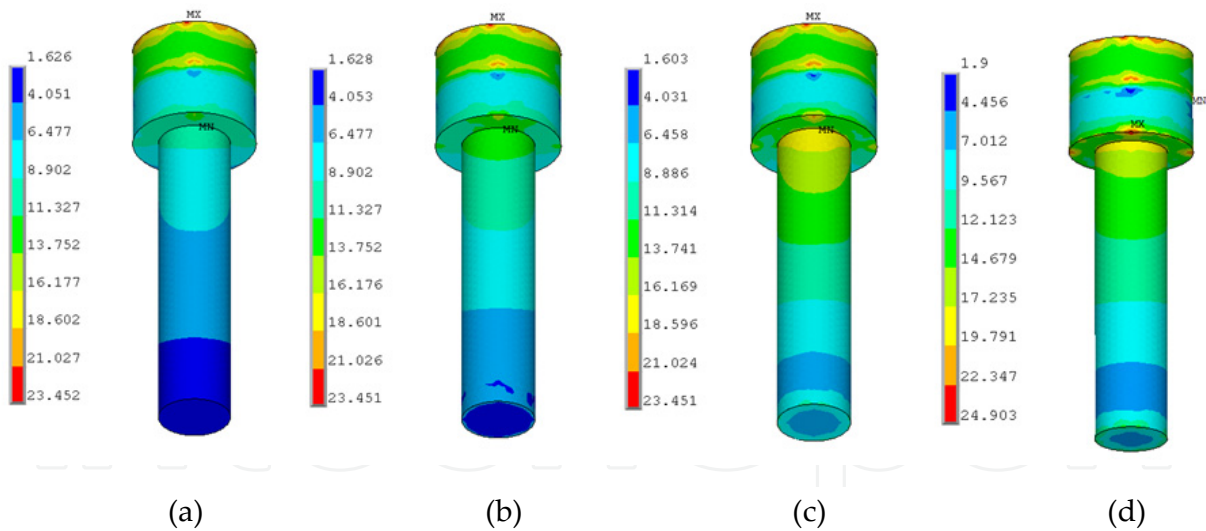(a)   (b)   (c)   (d)

Figure 10. Stress distribution in dense body of different modulus implants No.2: (a)80%; (b)40%; (c)10%; (d)1.3%

3.3. Effect of thickness of low modulus zone on the interface stress distribution of implant No.2

In order to further optimize the structure of the implant, the effect of thickness of low modulus zone on the interface stress distribution of implant No.2 was carried out, by

varying the thickness of the low modulus zone from 0.5, 0.75, 1 to 1.25mm and maintaining the same implant diameter of 4.1mm and a constant modulus of low modulus zone, i.e.1370MPa. Figure 11 represents the stress distribution at the implant-bone interface in the axial direction. It can be seen that, in all cases, the cortical bone are in high stress zone while the cancellous bone are in low stress zone. The change of the thickness of low modulus zone affects the stress distribution of cancellous bone a lot while it has little influence on cortical bone, as shown in Fig.12. With the increase of the thickness, the interface stress decreases, especially in the root apex. Moreover, the distribution of the interface stress becomes more uniform. When it comes to an optimal thickness suitable for the clinical application, the strength and ingrowth of the bone tissues should be considered, which need further verification of MADIT experiments.
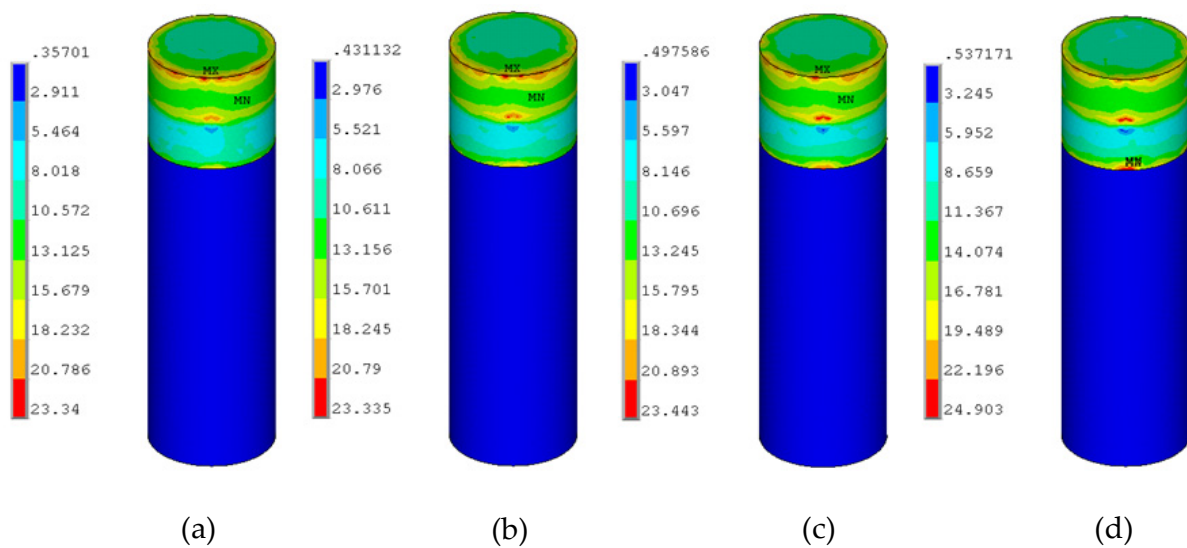

(a)   (b)   (c)   (d)

Figure 11. Stress distribution in axial direction ata implant-bone interface of implants No.2 with different thickness of low modulus layer: (a)0.5mm;(b)0.75mm;(c)1mm;(d)1.25mm
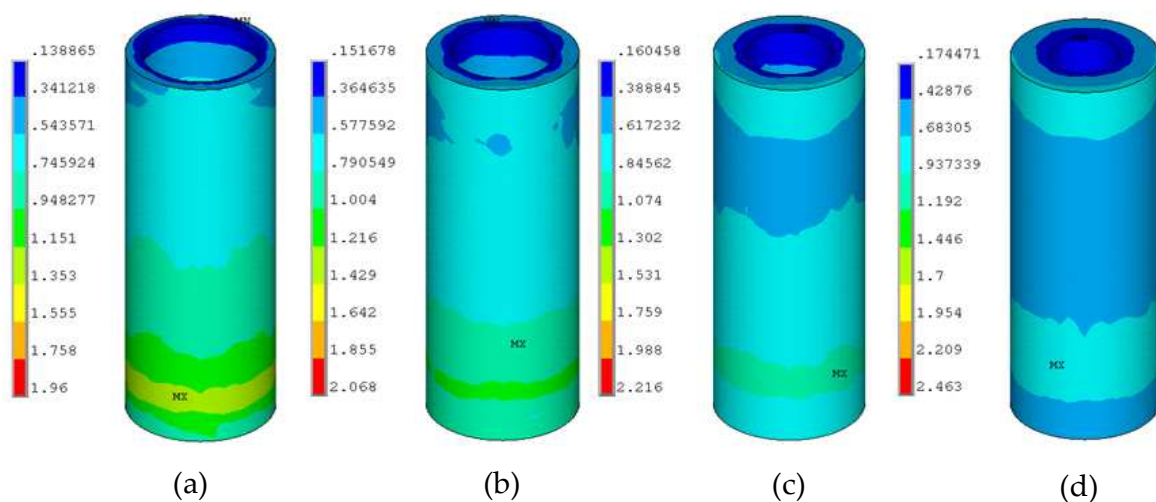

(a)   (b)   (c)   (d)

Figure 12. Stress distribution at cancellous bone interface of implant No.2 with different thickness of low modulus layer:(a)0.5mm;(b)0.75mm;(c)1mm;(d)1.25mm

3.4. Stresses distribution on implant-bone interface under static and dynamic loading conditions

In order to compare the Von Mises stresses of the sense implant with that of the bio-mimetic implant under dynamic loading and static loading stations, the model structures of NO.1 and NO.2 are designed in the same way. The elasitc modulus of NO.1 and NO.2 dense body both are 103.4Gpa,that of NO.2 porous layer is 41.36Gpa, the poisson ratio of all three is 0.35.

3.4.1. Maximum stresses

As shown in table 6, the maximum stresses under dynamic loading conditions were 17.15% higher than that under static loading conditions. The maximum stresses in cortical bone of two implants were similiar. However, the maximum stress of the dense implant was 75.79% high than that of the bio-mimetic implant in spongy bone, and 22.46% higher in the root region. The maximum stresses at implant-bone interface were much smaller than the yield strength of pure titanium (462MPa).

Loading region	Maximum Von Mises stresses (MPa)			
	No.1 static	No.1 dynamic	No.2 static	No.2 dynamic
Cortical bone region	15.265	17.884	15.264	17.882
Cancellous bone region	9.962	11.671	5.661	6.632
Root-end region	4.973	5.826	4.069	4.767

Table 6. Maximum Von Mises stresses of the dense implant and the bio-mimetic implant under static and dynamic loading conditions

3.4.2. Stress distribution within the cortical bone surrounding the implant neck and in implant-bone interface of implants No.1 and No.2 in static and dynamic loading

Figure. 13 represent the stress distribution within the cortical bone surrounding the implant neck. The maximum stress occurred at the edge of the cervical cortical bone of implant No.2 were greater than those of implant No.1. For No.2, the maximum stresses were 7.192MPa in static loading condition and 8.428MPa in dynamic loading condition. For No.4, the maximum stresses were the maximum stresses were 6.67MPa in static loading condition and 7.814MPa in dynamic loading condition. The results indicated the implant No.2 had 7.85% and 7.67% higher stresses than the implant No.4 in dynamic and static loading conditions, respectively. The maximum stresses of the implant No.2 in static and dynamic loading conditions were only10.42% and 21.21% of the yield strength of cortical bone, 69MPa, respectively .

Figure.14 represent the stress distribution in the implant-bone interface in an axial direction. In both loading conditions, the maximum stresses at implant interfaces in the implant No.1

and 2 showed no difference in the cortical bone area, while the high stress zone of the implant No.1 was greater than that of the implant No.2 in the spongy bone area and around the root apex. The yield strength of pure titanium was 462MPa. In static and dynamic loading conditions, the maximum stresses of the implant No.2 at the interface were 15.264MPa and 17.882MPa respectively, and they were only3.3% and 3.87% of the yield strength of pure titanium.

Figure.15 represent the stress distribution in interface of spongy-bone implant. The stresses at the implant interface in dynamic loading condition were all higher than those in static loading condition. Both implant bodies had high stress zones in the junction of the cortical bone and spongy bone, and the stresses at the implant interface showed a declining trend from top to bottom but increased at the root apex. The interface stresses of the implant No.1 was higher than that of the implant No. 2, and the maximum stress at the bone interface of the implant No.1 was 75.97% higher than that of the implant No.2.
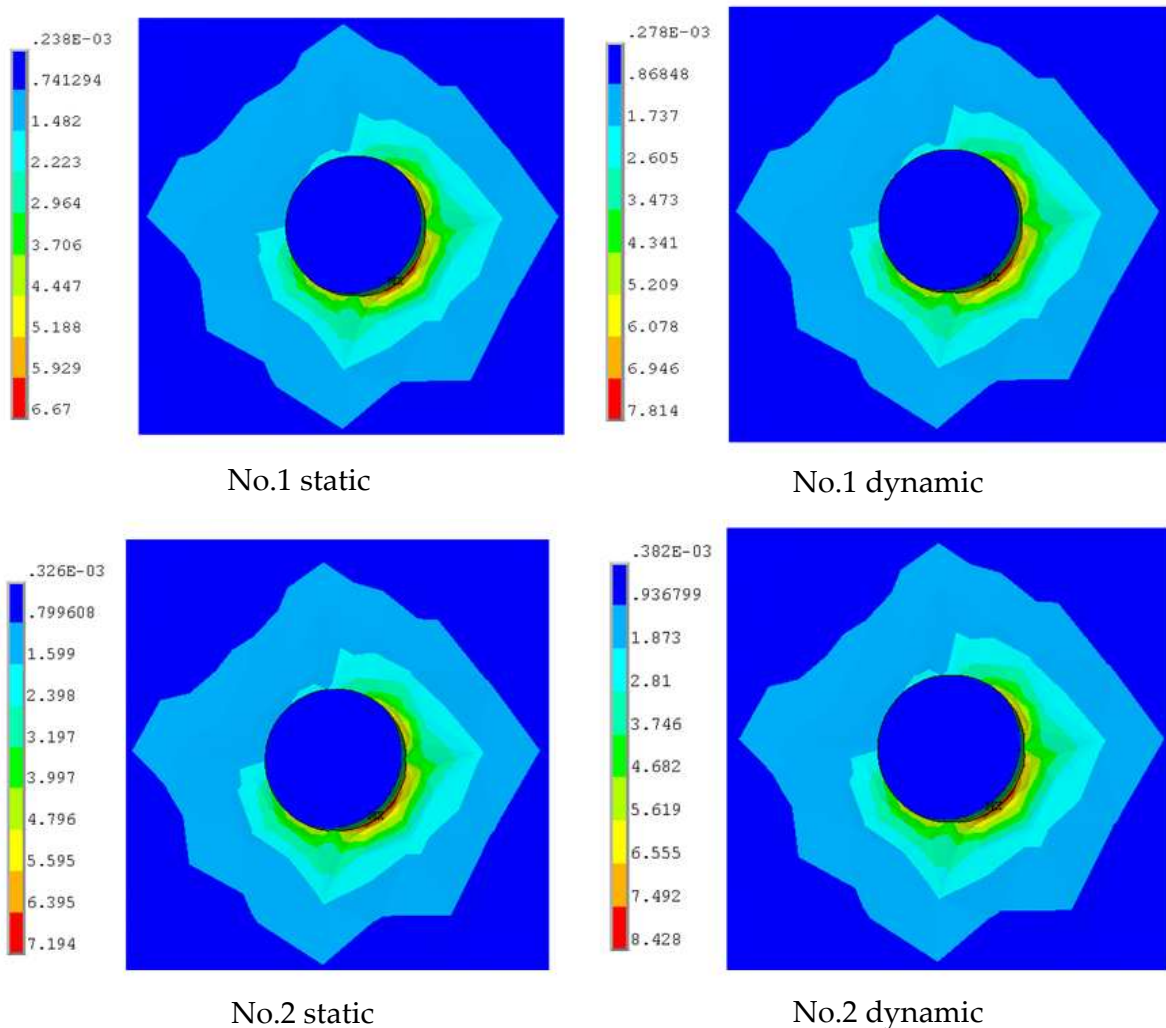

No.1 static   No.1 dynamic

No.2 static   No.2 dynamic

Figure 13. Stress distribution in the cortical bone of the implant No.1 and No.2 under static and dynamic loading conditions.

Figure. 16 represent the stress distribution in the dense body of the implants. There was a high stress zone of the dense body in the junction of the porous layer and the dense body of the implant No.2. The maximum stress of 12.306MPa in dynamic loading condition was higher than that of 10.504MPa in static loading condition. In the spongy bone area, the high stress zone of the dense body of the implant No.2 was greater than that of the implant No.1. The yield strength of pure titanium was 462MPa; the maximum stress at the interfaces of implant dense body did not reach the yield strength of pure titanium.
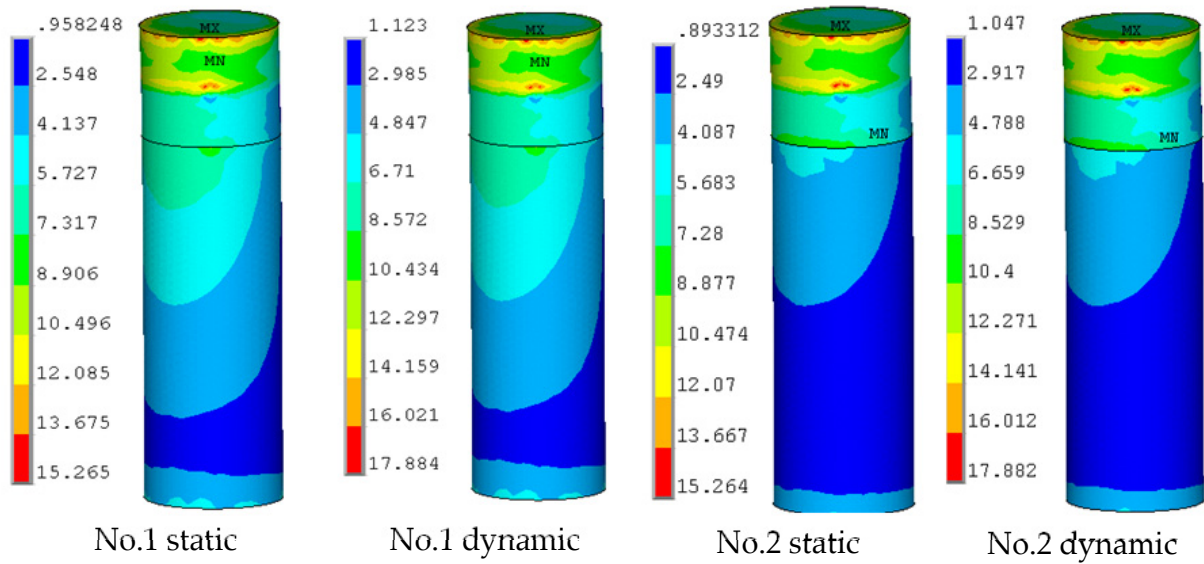

No.1 static   No.1 dynamic   No.2 static   No.2 dynamic

Figure 14. Stress distribution in the bone-interface of the implant No.1 and No.2 under static and dynamic loading conditions

No.1 static   No.1 dynamic   No.2 static   No.2 dynamic

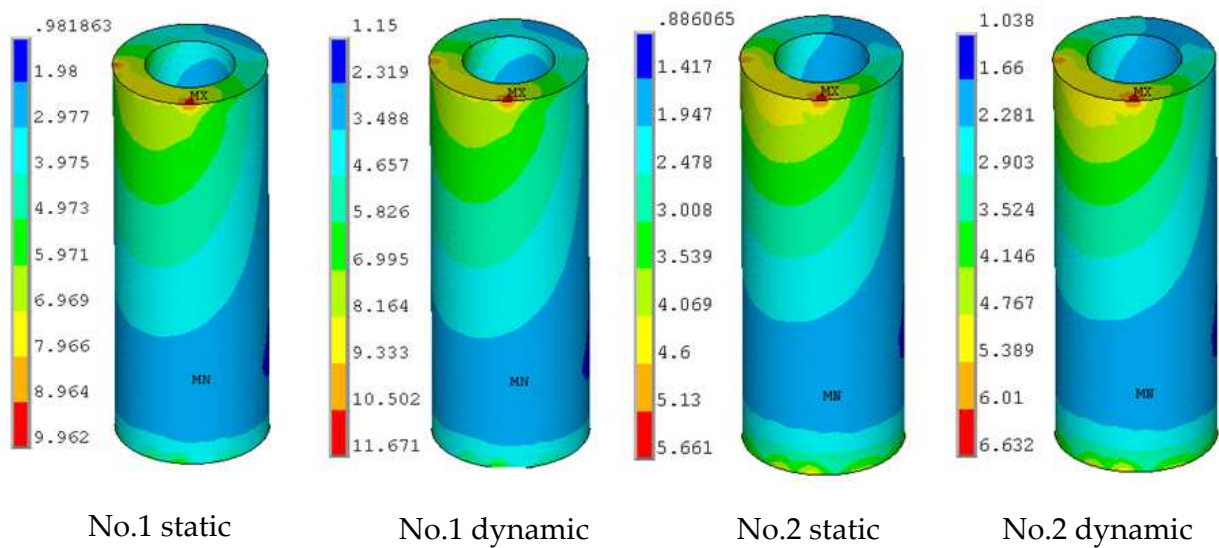**Figure 15.** Stress distribution in the spongy bone-interface of the implant No.1 and No.2 under static and dynamic loading conditions

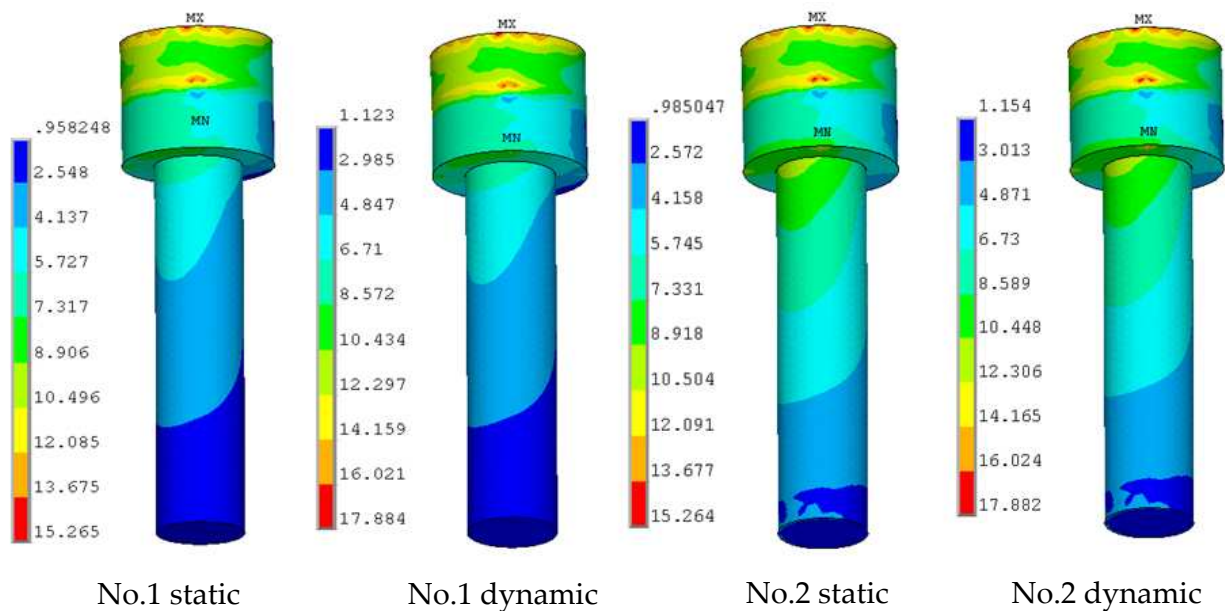| No.1 static | No.1 dynamic | No.2 static | No.2 dynamic |

Figure 16. Stress distribution in the dense body of the implant No.1 and No.2 under static and dynamic loading conditions

3.4.3. Fatigue analysis of bio-mimetic implant

In the fatigue calculations, referring to the fatigue curves of pure titanium (S-N curves) shown in Figure 5, the fatigue life of implant was calculated based on Goodman, Soderberg, Gerber and Mean-Stess fatigue theories and formulas which were illustrated in Table 3. The endurance limit of pure titanium (Se) is 259.9MPa, and the yield strength (Sy) is 462MPa. The safety factors of different dense bodies of bio-mimetic implants with dynamic preload were calculated using the Soderberg formula in Table 3, as shown in Figure. 17. Figure. 17 represent the safety factors of different dense bodies of bio-mimetic implants when the dynamic preload was applied. Under an axial force of 50~300N and a lingual force of 45°25N in dynamic loading condition, the safety factors of dense body were all above 10. The results show that the bio-mimetic implant is safe against fatigue load.

Figure 18 showed the maximum stress at the interface of porous layer and the bone under different preloading conditions. With the increase of the loading, the interface stress of porous layer linearly increased. In dynamic loading condition with normal chewing force (axial 150N and lingual 45°25N), the maximum stress at the porous layer interface (σmax) was 6.632MPa, and the minimum (σmim) was 1.038MPa. When an axial force of 300N and a lingual force of 45°25N were applied, the maximum stress at the porous layer interface (σmax) was 11.38MPa, and the minimum (σmim) was 1.97MPa. According to the simulation results, it was predicted that the strength of the porous layer of the bio-mimetic implant and its bonding strength with the dense body interface should both be greater than the maximum interface stress (11.38MPa), which ensured the implant safety. The analyses of the implant interface stress provide a basis of mechanical properties for the preparation of porous layer of bio-mimetic implant.
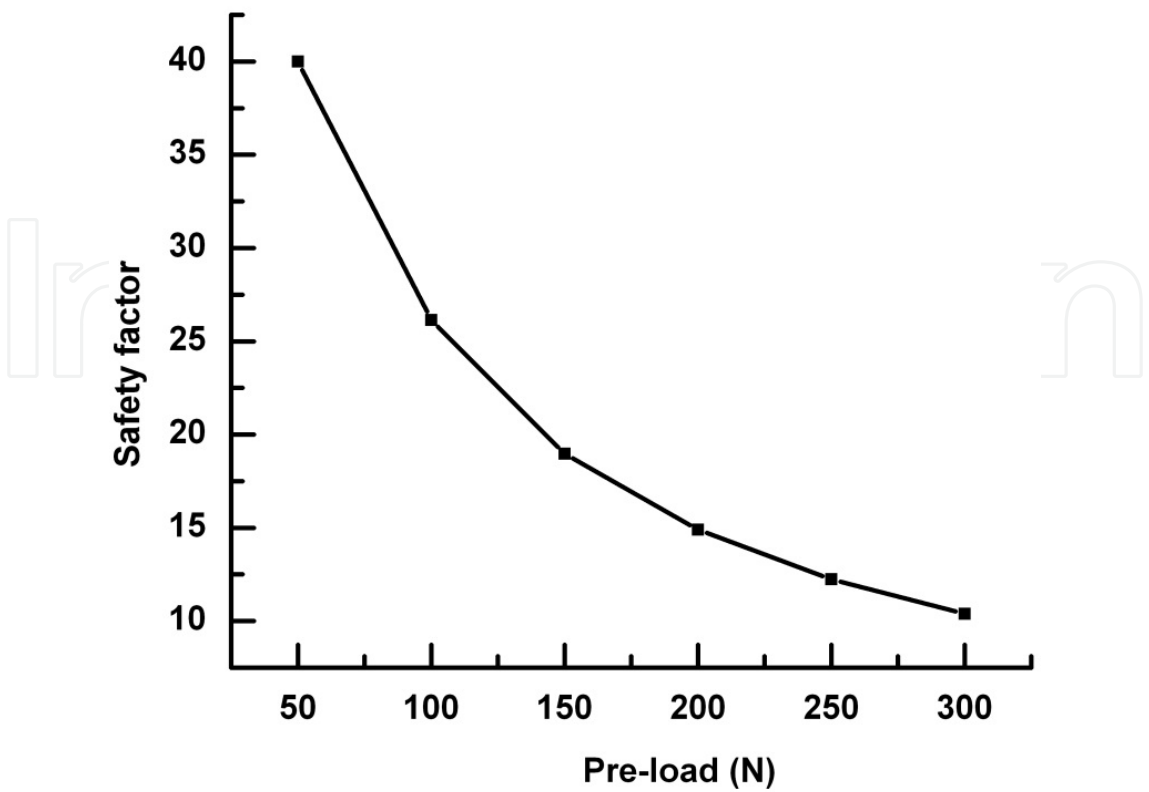
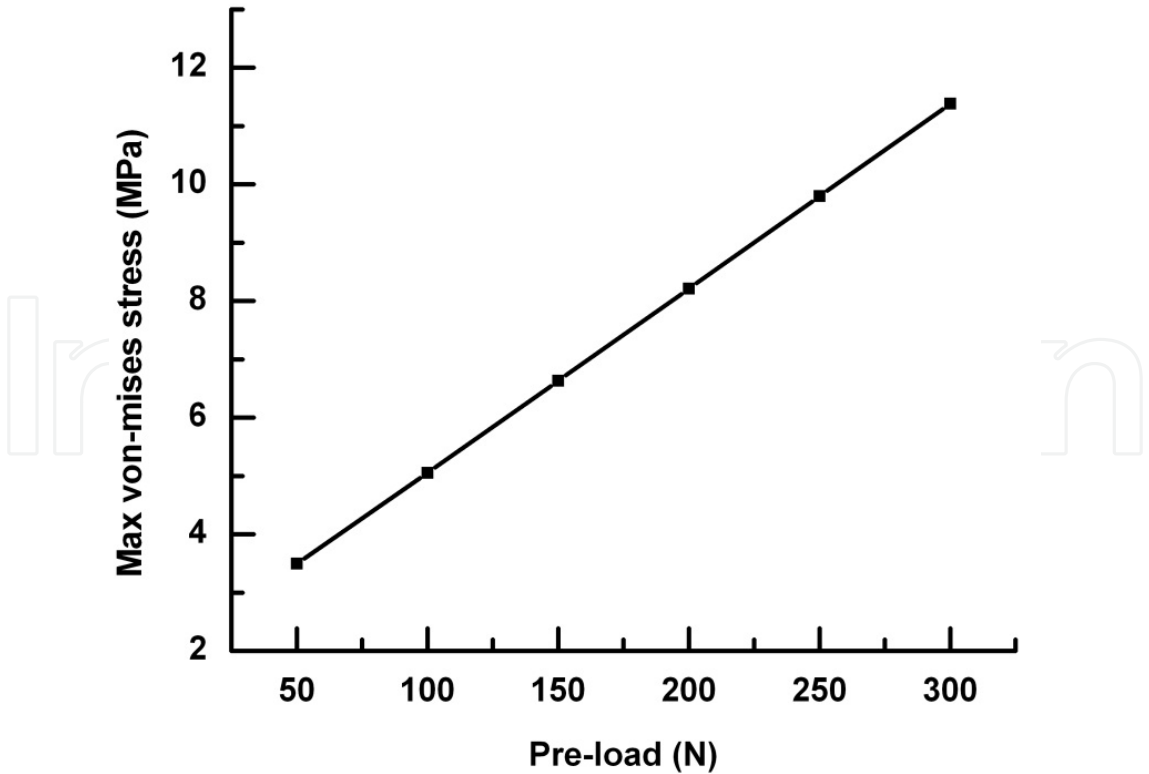**Figure 17.** Safety factor for dense body of bio-mimetic implant under different dynamic loading

Figure 18. Maximum Von-mises stress for bone-interface porous layer of implant under different dynamic loading conditions.

4. Discussion

The functions of implant are mainly dependent on the direct bonding with the surrounding bones. The long-term success of an implant is determined by the reliability and stability of the implant bone interface, and the success or failure of an implant is determined by the manner that the stresses at the bone-implant interface transfer to the surrounding bones[1, 2]. The main factors contributing to the stability of implants include the structure of the implants, the distribution of the interface stress and the combination mode of the interface. In order to ensure the long-term stability of an implant, the implant should be designed according to two main principles. First, the load should be minimized to avoid exceeding its physiological tolerance as overloading can cause bone resorption or fatigue failure of the implant. On the other hand, underloading may lead to disuse atrophy and subsequent bone loss[3, 4]. Second, the contact zone with the bone should be increased to reduce the bone interface stress. The structural characteristic of the mandible shows an outer layer of dense cortical bone and an inner layer of loose cancellous bone. Both the elastic modulus and mechanical strength of cortical bone (10~18GPa) are higher than those of cancellous bone (1.3~4GPa). Current dense implants do not have the structure similar to that of the mandible, as well as modulus. As a result, the mechanical compatibility between the implant and the bone remains unresolved, and the modified active coating on the surface gets easily damaged in the implantation process. An implant with a low elastic modulus is believed to be beneficial to transferring the stress to the surrounding bones, resulting in a long-term stability[8,9]. The porous implant materials can tremendously improve the implant biocompatibility [10-12] by improving the adhesion and outgrowth of those osteoblasts, promoting the deposition of extracellular matrix, increasing the adsorption of nutrients and oxygen, and promoting the new bones' growth into pores to achieve biological fixation. The porosity can be changed to adjust the density, strength and elastic modulus of the material to achieve similar mechanical properties to the replaced hard tissues. Meanwhile, the porous structure can provide scaffold for the bioactive coating to promote osseointegration. In this study, according to the structural characteristics of the mandible and the advantages of the porous implant material, an idea of a bio-mimetic implant is proposed. It is a titanium implant composed of a cortical bone zone with a dense structure and a cancellous bone zone with a porous outer layer and a dense body. The cortical bone has a high modulus, and the porous outer layer of the cancellus bone zone has a low modulus. The dense body ensures the strength to meet the requirements of clinical applications. To optimize the structure of the bio-mimetic implants, the finite element analysis was carried out. The effects of implant structure, modulus and thickness of the low modulus layer on the distribution of the interfacial stress were studied.

The interfacial stress of the implants is mainly located at the interface between the implants and the surrounding bones,affecting the interface biological reactions such as bone resorption and remodeling. Cortical bone loss and early implant failure after loading are usually accompanied by the excess stress at the implant bone interface while a low stress

may lead to disuse atrophy and subsequent bone loss [13,14]. It is indicated that, under the same situation, the smaller the bone surface area in contact with the implant body is, the greater the overall stress becomes [15]. Cortical bone, which has a higher modulus, higher strength and more resistance to deformation than cancellous bone [16], can bear more loading in masticatory movements [17-20]. In this study, it was supposed that the implant-bone osseointegration was 100%. Under the same loading condition, the stress distributions at the interface of four different structure implants were compared and analyzed, showing the change of the implant structure and modulus in the cancellous bone had significant effects on the stress distribution. In all cases, there are high stress zone at the interface between cortical and cancellous bone. In cancellous bone, the interface stress decreases from top to bottom, and increases at the root apex.

In the cortical bone zone, all implants present high stress values and the maximum stresses are in the same level. In the cancellous bone zone, the maximum stress of the dense implant interface was 75.58% higher than that of the bio-mimetic implant, and 22.21% higher than that in the root apex zone. The maximum stresses in cancellous bone and root region of implant No.2 are lower than those of other three implants. The maximum stress of implant No.4 is 42.96% higher than that of No.2. Implant No.3 has the highest stresses in root region. The stress distribution at bone-implant interface varied with elastic modulus of low elastic modulus layer. The maximum stresses of implant No.2 decreases with the decreasing of elastic modulus in cancellous bone region, while there is no significant difference in cortical bone region. When the modulus of the low modulus layer is reduced to 10% of the dense ones, a uniform distribution of interfacial stress without any high stress zone was obtained. With the increase of the thickness of the low modulus layer, the interface stress decreases, especially in the root apex. Moreover, the distribution of the interface stress becomes much uniform.

From the biomechanical point of view, a structure like implant No.2, a modulus matches the cancellous bone and a suitable thickness can effectively reduce the stress in the implant-bone interface and be beneficial to the transfer of interfacial stress to surrounding bones, which is favorable to the long-term stability of the implant. The structural characteristics of this implant are in line with those of the mandible, so that the elastic modulus of the porous zone can be reduced to make the elastic modulus of the implant match with that of the cancellous bone and thus help the interface stress tranferring. The structural characeristics of mandible of implants No.1and No.4 are ingored, which results in the un-uniform interface stress distribution and stress concentration in cancellous bone. Although implant No.3 has a mandible –like structure, the cancellous bone is a whole low modulus structure, which leads to stress concentration at both interface and root apex.

Implant No.2 has a low modulus-outer and high modulus-interior in the cancellous bone zone. The low modulus-outer can be realized by adjusting the porosity and pore size to match the mechanical properties, especially the elastic modulus, with the surrounding bones. Figure. 19 illustrates the stress distribution of the porous and dense implants under

vertical loading. In the model, R refers to the radius of the implant, H refers to the height, and F refers to the vertical loading. Assuming that the compressive stress and shear stress are uniform, and the compressive stress and shear stress on porous and dense implants are $\sigma 1$, $\tau 1$ and $\sigma 2$, $\tau 2$, respectively. The porous implants provide more contact area with the bone than the dense implants. Assuming that A1 is the added contact area, the equilibrium equations of forces for porous and dense implants can be expressed as:

$$F = (\pi R^2 + A_1)\sigma_1 + 2\pi R H \tau_1 \tag{1}$$

$$F = \pi R^2 \sigma_2 + 2\pi R H \tau_2 \tag{2}$$

Because the compressive strength at the interface is much larger than its shear strength, the values of $\sigma 1$ similar to $\sigma 2$, and the added zone A1 are larger, we can obtain $\tau 1 \ll \tau 2$. It means that the shear force of porous implants is much smaller that that of dense ones, which is beneficial for the stability of the low strength cancellous bone.
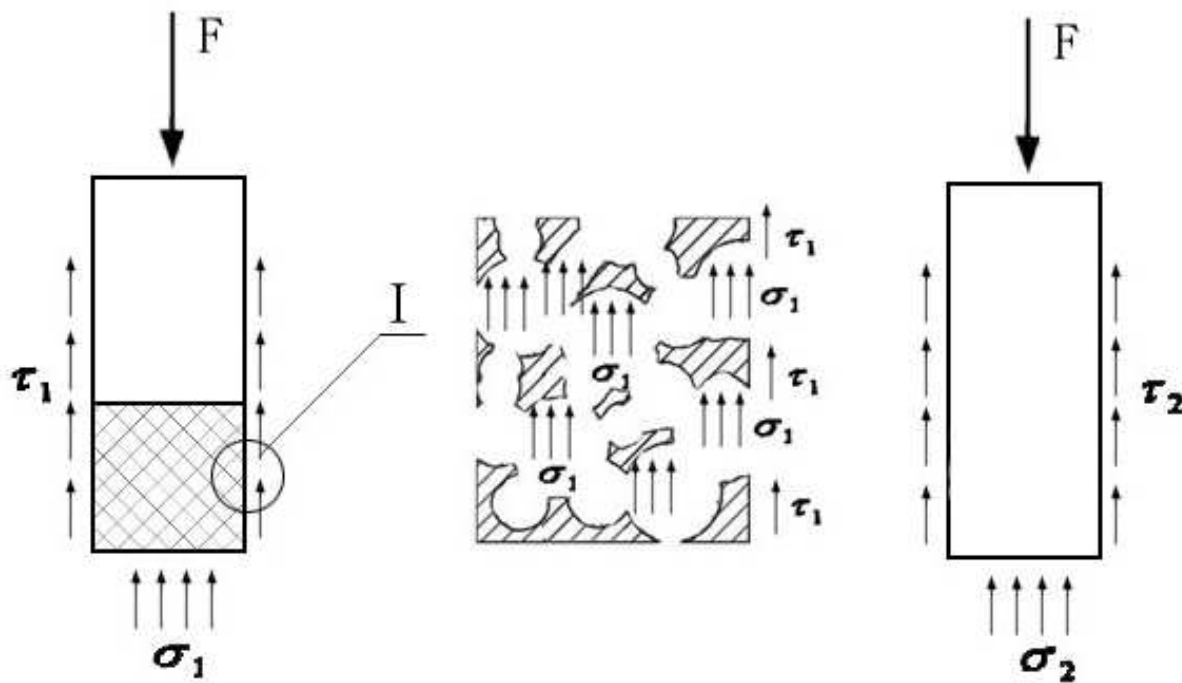

Figure 19. Stress analysis of implants

In current industry, a screw structure is usually adopted to improve the bond strength between the bone and implants. The modulus of screw zone is higher than that of cortical bone, which has a high trend to cause stress shielding and concentration and thus bone absorption [21]. For a porous structure, when the bone tissue grows into the porous structure, the bond strength is improved and the modulus of implants is similar to that of the surrounding bones. No bone absorption occurs under loading because part of the stress can be borne by bone tissues in the pore. In summary, biomimetic style implant No.2, with a high modulus in the cortical bone and low modulus-outer and high modulus-interior in the

cancellous bone is superior in the stress teansferring. The porous structure can effectively reduce the shear force at the bone-implant interface, providing a suitable environment for bone tissue ingrowth, which is benefit for the longtime stability of the implants.

5. Conclusions

1. The distribution of interface stress is strongly depended on the structure of the implants. The bio-mimetic implant No.2 is favorable to transferring the interface stress from the cancellous bone and root apex bone to surrounding bones, avoiding stress shielding and concentration.
2. It is demonstrated that the interface stress varies significantly with the change of the modulus of the low modulus layer. The area of the high stress zone is reduced, and the value of the interface decreases dramatically. When the modulus of the low modulus layer is reduced to 10% of the dense value, a uniform interface stress distribution without any high stress zone was obtained.
3. The change of the thickness of low modulus zone affects the stress distribution of cancellous bone, while it has no significant influence on cortical bone. With the increase of the thickness, the interface stress decreases, especially in the root apex. Moreover, the distribution of the interface stress becomes much uniform.

Author details

Chen Liangjian
The Third Xiangya Hospital of Central South University, ChangSha, China
State Key Laboratory of Powder Metallurgy Central South University, ChangSha, China

6. References

[1] Van Osterwyck H, Duyck J, Vander S, Vander PG, Decoomans M, Lieven S, Puers R, Naert L. The influence of bone mechanical properties and implant fixation upon bone loading around oral implants [J]. Clin Oral Implants Res, 1998, 9(6):407-412.
[2] Geng J, Tan K B C, Liu G. Application of finite element analysis in implant dentistry: a review of the literature [J]. J Prosthet Dent, 2001, 85(6):585–598.
[3] Vaillancourt H, Pillar RM, McCammond D. Factors affecting cortical bone loss with dental implants partially covered with a porous coating: a finite element analysis[J]. Int J Oral Maxillofac Implants, 1996, 11(11):351–359.
[4] Pilliar RM, Deporter DA, Watson PA, Valiquette N. Dental implant design effect on bone remodeling[J]. J Biomed Mater Res, 1991, 25(4):467–483.
[5] Bathe KJ. Finite element procedures[M]. Upper Saddle River (NJ): Prentice-Hall; 1996. p. 148–377.

[6]   Sato Y, Wadamoto M, Tsuga K, Teixeira ER. The effectiveness of element down sizing on a three-dimensional finite element model of bone trabeculae in implant biomechanics[J]. J Oral Rehabil ,1999;26:288–91.

[7]   Sahin S, Cehreli MC, Yalcm E. The influence of functional forces on the biomechanics of implant-supported prostheses—a review[J]. J Dent,2002; 20:271–82.

[8]   Kayabas O , Yu¨zbasıog˘lu E , Erzincanli F. Static, dynamic and fatigue behaviors of dental implant using finite element method [J]. Advances in Engineering Software, 2006, 37(10):649–658.

[9]   Meijer GJ, Cune M S, Vandooren M. A comparative study of flexible (polyactive versus rigid hydroxyapatite) permucosal dental implants: clinical aspects[J]. J Oral Rehabil, 1997, 24(2): 85-88

[10] St-Pierre J P, Gauthier M, Lefebvre LP, Tabrizian M. Three-dimensional growth of differentiating MC3T3-E1 pre-osteoblasts on porous titanium scaffolds [J]. Biomaterials, 2005, 26(35):7319–7328.

[11] Otsukia B, Takemotoa M, Fujibayashia S, Neo M, Kukubo T, Nakamura T. Pore throat size and connectivity determine bone and tissue ingrowth into porous implants: Three-dimensional micro-CT based structural analyses of porous bioactive titanium implants[J]. Biomaterials, 2006, 27(35):5892–5900.

[12] Takemoto M, Fujibayashi S, Neo M, Suzaki J, Kukubo T, Nakamura T. Mechanical properties and osteoconductivity of porous bioactive titanium[J]. Biomaterials, 2005, 26(30): 6014–6023.

[13] Misch CE. Contemporary implant dentistry [M]. 2nd ed. St. Louis: Mosby; 1998. p. 109–34, 207–17, 329–43, 595–608.

[14] Schroeder A. Oral implantology: basic, ITI hollow cylinder system [M]. New York: Thieme Medical Publishers; 1996. p. 60–65.

[15] Holmes DC, Loftus JT. Influence of bone quality on stress distribution for endosseous implants [J]. J Oral Implantol 1997;23(3):104–111.

[16] Misch CE. Density of bone: effect on treatment plans, surgical approach, healing, and progressive bone loading [J]. Int J Oral Implantol ,1990;6(2):23–31.

[17] Cochran DL. The scientific basis for and clinical experiences with Straumann implants including the ITI dental implant system: a consensus report [J]. Clin Oral Implants Res ,2000;11(11):33–58.

[18] Lekholm U, Zarb GA. Tissue-integrated prostheses [M]. In: Branemark PI, Zarb GA, Albrektsson T, editors. Tissue-integrated prostheses. Chicago: Quintessence; 1985. p. 199–209.

[19] CHEN Liang-jian, LI Yi-min. Influence of structure and elastic modulus of titaniun implant on implant-bone interfacial stress distribution[J]. Journal of Central South University(Science and Technology), 2009, 40(2):400-405.

[20] CHEN Liang-jian,GUO xiao-ping, LI Yi-min, LI Ting. Finite element analysis for interfacial stress and fatigue behaviors of bio-mimetic titanium implant under static and dynamic loading conditions. J cent south univ (Med sci),2010, 35(7):662-672.

[21] Gefen A. computational simulations of stress shielding and bone resorption around existing and computer-designed orthopaedic screws[J]. Medical and Biological Engineering and Computing, 2002,40(3): 311-322.